ELSEVIER

Polymer 42 (2001) 8395–8405

polymer

www.elsevier.nl/locate/polymer

Melting and morphology in melt-crystallized *meta*-linked poly(aryl ether ketone)

L.L. Chang, B.S. Huang, E.M. Woo*

Department of Chemical Engineering, National Cheng Kung University, Tainan 701-01, Taiwan, ROC

Received 18 December 2000; received in revised form 7 May 2001; accepted 14 May 2001

Abstract

Unique thermal behavior and accompanying morphology in *meta*-linked poly(ether diphenyl ether ketone) (PEDEK*m*) melt-crystallized at various conditions was analyzed. The two widely spaced and well-resolved melting peaks ($T_{m,1}$ and $T_{m,2}$) in PEDEK*m* offered a unique model for proposing a more advanced interpretation on the complex and highly controversial issues of multiple melting and crystalline morphology commonly seen in semi-crystalline polymers. There are two main lamella types of different thickness populations, whose melting peaks labeled P1 and P2 may appear in series giving two melting endotherms at 302 and 322°C, respectively. However, despite the series appearance of two melting peaks upon scanning, only one type of lamellae preferentially exists in the melt-crystallized PEDEK*m* depending on processing temperatures/histories. When isothermally crystallized at lower temperatures (290°C or lower), PEDEK*m* possesses only the P1 crystal, which may or may not be melted/re-crystallized into thicker P2 crystal entity depending on heating rates or annealing temperature/time. A break-off temperature for lamellar thickness in PEDEK*m* is about 300°C. When crystallized at 300°C or higher, PEDEK developed only the P2 crystal, which is mainly a thickened and branched axialite. This study also demonstrated that the unit cell remained unchanged for either the P1 or P2 crystal entities. © 2001 Published by Elsevier Science Ltd.

Keywords: Aryl ether ketone polymer; Melt crystallization; Multiple melting

1. Introduction

Polyetherketone polymers have been widely studied. Among the many subjects, thermal properties and relationships with crystalline morphology are especially interesting and critical issues [1–11]. The general structure of polyetherketone-type polymers contains phenyl or biphenyl groups linked by ether (–O–) or ketone (–CO–) groups in the *para*- or *meta*-positions of aromatic rings. The ether/ketone ratio is a structural parameter that has been often studied to correlate with the crystalline morphology. Gardner et al. [1,2] have studied polyketones containing isophthalic vs. terephthalic units. They have claimed that for aryletherketone polymers of carbonyl contents greater than 50%, cold-crystallization or solvent-induced crystallization showed a second crystal form different from the regular orthorhombic unit cell. Blundell and Newton [12] observed that for polyketones containing carbonyl contents larger than 50% (i.e. ether/ketone ratio < 1), an additional crystal form was found with same orthorhombic packing except for exchanged *a*, *b* dimensions. Cheng et al. [4,5] also reported polymorphism (orthorhombic forms I, II, III) in poly(ether ketone ketone)s with terephthalic- (T), isophthalic- (I), or (T/I) linkages. Poly(ether ether ketone) (PEEK), with ether/*ketone* > 1 and all *para*-linkages, is probably the most studied system. Olley et al. [13] conducted an early spherulitic morphology study on PEEK using SEM coupled with an etching technique. Lovinger et al. [14] have conducted detailed morphology studies on PEEK using electron diffraction, SEM, X-ray diffraction, etc. and gained much insight of the crystalline structures. Marand et al. [7] conducted similar studies on PEEK and claimed that double melting is associated with a second type of crystal structure evolving from higher crystallization temperature beyond 300°C. *para*- vs. *meta*-linkage in the polyketone polymers is another structural parameter. Unusual melting and crystallization in *meta*-phenylketone-ether polymers have been reported and various interestingly probing interpretations have been offered. Rueda et al. [8–10] claimed that both *meta*-linked oligomeric poly(ether ether *meta*-ketone) and *para*-linked poly(ether ketone ether ketone ketone) (PEKEKK) contain two crystalline phases, exhibiting two melting endotherms. In an opposite view, Blundell et al. [3] and Wang et al. [11]

---

* Corresponding author. Tel.: +886-6-275-7575, ext. 62670; fax: +886-6-234-4496.

E-mail address: emwoo@mail.ncku.edu.tw (E.M. Woo).

0032-3861/01/$ - see front matter © 2001 Published by Elsevier Science Ltd.
PII: S0032-3861(01)00346-9

conducted studies on a *meta*-linked poly(ether diphenyl ether ketone) (PEDEK*m* or commercially known as PK-99), but found no difference in the unit cell. Dramatically and contradictory views of interpretations on multiple melting have been proposed; apparently, relationships between thermal behavior and morphology in polyketone-type polymers need further clarification.

Thermal behavior and crystalline morphology in semi-crystalline polymers are complex and usually exhibit double melting or even multiple melting in addition to an 'annealing peak' that is located 10–20°C above the temperature at which the polymers are isothermally crystallized or annealed. Various interpretations include mechanisms of re-organization or melting/re-crystallization (upon scanning or annealing) [15–17], different lamellar morphologies [3,6], or simultaneous existence of different crystal entities [5,7]. A more complex combination may also be possible, e.g. melting/re-crystallization mechanism coupled with existence of different unit-cell crystals, as recently demonstrated in syndiotactic polystyrene (sPS) showing four sharp melting peaks that are associated with two different unit cells [18].

The melting behavior of PEDEK*m* is similar to that for the *meta*-linked or *para*-linked PEKEKK in that they all exhibit two distinctly separate low-melting and high-melting peaks. It has been reported for PEDEK*m* that a higher-melting peak appeared at about $T_{m,2} = 322°C$ following the endotherm of a lower-melting crystal entity of $T_{m,1} = 302°C$. It is critical to discern relationships between the crystal entities of $T_{m,1}$ vs. $T_{m,2}$ and circumstances under which the crystal entity of $T_{m,2}$ can be developed more favorably than the crystal entity of $T_{m,1}$ or vice versa. PEDEK*m* has been studied from perspectives of crystallization from the amorphous rubbery state and subsequent thermal transitions of PEDEK*m* and their relationships with its developed crystalline morphology were investigated in some earlier reports [8–11]. Interpretation of lamellar morphology from melt-crystallization of the polymer has been less reported. This study focused on probing behavior of the polymer as it formed crystals from melt-crystallization. The main objective of this study was thus concerning elucidation of crystal/lamellar morphology in relation with the observed melting/crystallization behavior in melt-crystallized PEDEK*m*. The two widely spaced and well-resolved melting peaks ($T_{m,1}$ and $T_{m,2}$) in PEDEK*m* allowed unambiguous and more rigorous analyses for proposing a more advanced interpretation on the complex and highly controversial issues of multiple melting and crystalline morphology commonly seen in semi-crystalline polymers.

2. Experimental

2.1. Materials and procedures

The synthesis of PEDEK*m* was performed in this laboratory by following the procedures earlier reported in literature [19]. The procedures will not be repeated here. The diphenylsulphone solvent and residual salts in the final polymerized product were carefully removed by leaching repeatedly (several times), first with 200 ml acetone (20°C), and then with water (80°C). The polymer was dried at 120°C under vacuum. The final yield (after leaching and purification) was found to be 85 wt%. T_g of the synthesized PEDEK*m* was found to be 155°C (onset) and an apparent T_m of 308°C (peak), in general agreement with the literature values (measured by DSC at 20°C/min). For reference, the chemical structure of PEDEK*m* is shown as following:

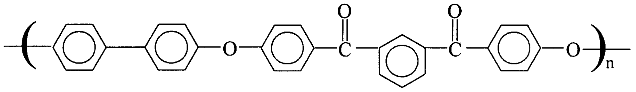

2.2. Apparatus

Thermal characterization (crystallization, melting, enthalpy) of the samples were performed using a differential scanning calorimeter (DSC, Perkin–Elmer DSC-7) equipped with an intracooler and a computer for data acquisition/analysis. Various heating rates were used as necessary, which ranged from 2, 5, 10, 20, to 40°C/min. Peak temperatures and enthalpy of crystallization/melting were measured values at scan rates as specified in figures or texts.

The spherulitic/lamellar morphology of samples was examined using a scanning electron microscope (SEM, Philips XL-40FEG). Etching by 2% potassium permanganate in $H_3PO_4 + H_2SO_4$ (1:2) solution (24 h at ambient) was performed to enhance the crystalline/amorphous contrast. The washed/dried samples were then coated with gold by vapor deposition using a vacuum sputter prior to SEM characterization. In addition, a polarized-light optical microscope (Nikon Optiphot-2 POL) with a microscope heating stage (Linkam THMS-600 with TP-92 temperature programmer) was used to examine the spherulite structure. Thin films of polymer samples were deposited on glass slides. Subsequently, desired thermal treatments were performed on the programmed heating stage. Care was exercised in ensuring temperature accuracy and rapid equilibrium at desired temperatures for isothermal treatments.

Wide-angle X-ray instrument (WAXD) was Rigaku D/Max II-B with Cu Kα radiation and a wavelength of 0.1542 nm. For direct comparison and precise temperature control, specimens for X-ray characterization were prepared in the DSC cells using exactly same thermal treatments as described for the thermal analysis samples.

3. Results and discussion

3.1. Analysis of multiple melting peaks

Two sets of samples were prepared by melting the

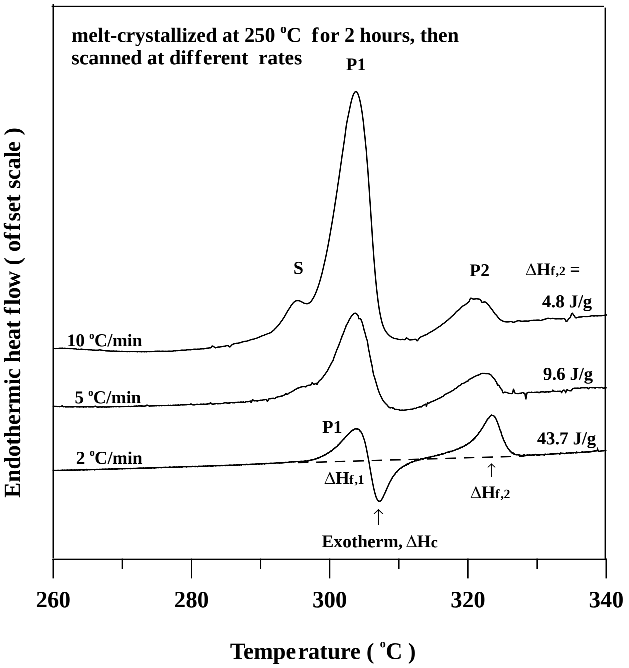

Fig. 1. DSC traces for 250°C-melt-crystallized PEDEK*m* scanned at (from bottom to top): 2, 5, or 10°C/min, respectively.

polymer (at 340°C) and letting it to crystallize (from melt) at a moderate temperature of 250 or 260°C, respectively. Note that the temperature window of fast crystallization for PEDEK*m* is about 250–260°C; thus, the melt-crystallization temperature of 250°C would proceed rather quickly, reaching a nearly maximum crystallinity within ca. 10 min. To ensure complete maximum crystallinity, the samples were held at 250°C for 2 h. The 250°C-melt-crystallized samples were then scanned from 250 to 340°C in DSC at 2, 5, and 10°C/min, respectively, to reveal the thermal transitions (melting, re-crystallization, re-melting, etc.). Fig. 1 shows the DSC result of the 250°C-melt-crystallized samples scanned at (from bottom to top): 2, 5, or 10°C/min, respectively. Interestingly, the slower scanning rates at 2 or 5°C/min revealed two wide-separated endotherms in the samples, which are possibly related to two distributions of crystal entities in the samples. The crystal entity associated with the first doublet-endotherm is hereby labeled as SP1 (shoulder peak + P1), whose peak melting is termed as $T_{m,1}$. The first melting doublet (SP1) is clearly composed of a minor shoulder peak (S) located at 296°C (when scanned at 10°C/min) and a major peak (P1) at ca. 304°C (when scanned at 10°C/min). The shoulder peak is less visible (merged with the major peak) for the melt-crystallized sample scanned at 2°C/min, but quite apparent (partially merged with the major peak) for the sample scanned at 10°C/min or higher. The DSC traces show that immediately after the melting endotherm of SP1 (at 300°C), an exotherm is located at about 307°C. This exotherm becomes increasingly significant for the samples scanned at the slowest rate (2°C/min). Origin of this exotherm may be related to either crystallization of still amorphous chains or re-crystallization of the previous melted crystal, which most likely is the SP1 crystal that just melts at 304°C. After completion of this exothermic process, a high-temperature melting endotherm (at ~322°C) follows. The crystal of high-melting peak at or near ~322°C is labeled as P2, and its melting peak is termed as $T_{m,2}$. Note that this high-melting peak (P2) lags far behind the first doublet (SP1) endotherm. Higher DSC scanning rates (10°C/min or higher), on the other hand, revealed only a doublet endotherm (SP1) at 296–305°C, with P2 becoming gradually smaller or completely missing from the DSC traces. Interestingly, the amount of P2 apparently decreases with increasing scanning rates. Absence of P2 may be a result of the fact the time was not sufficient for melting/re-crystallization of SP1 crystal when the scanning rates were high. When scanned at lower scanning rates, the samples, after melting of SP1 at $T_{m,1}$, apparently had enough time to develop a noticeable amount of P2 crystal entity, which melts at $T_{m,2}$. Possible mechanisms between SP1 and P2 will be discussed in more details later after examining more relevant results.

Again, similar DSC analyses were performed on PEDEK*m* samples melt-crystallized at another temperature of 260°C. Crystallization time was the same (10 min) for all samples in this set. The 260°C-melt-crystallized samples were then scanned from 260 to 340°C in DSC, to reveal the thermal transitions (melting, re-crystallization, re-melting, etc.). Fig. 2 shows the DSC result of the 260°C-melt-crystallized samples scanned at various rates as indicated for each trace. The overall trend is briefly discussed here. Similar results were obtained in that lower DSC scanning rates revealed SP1 and P2 peak lagging behind, but higher

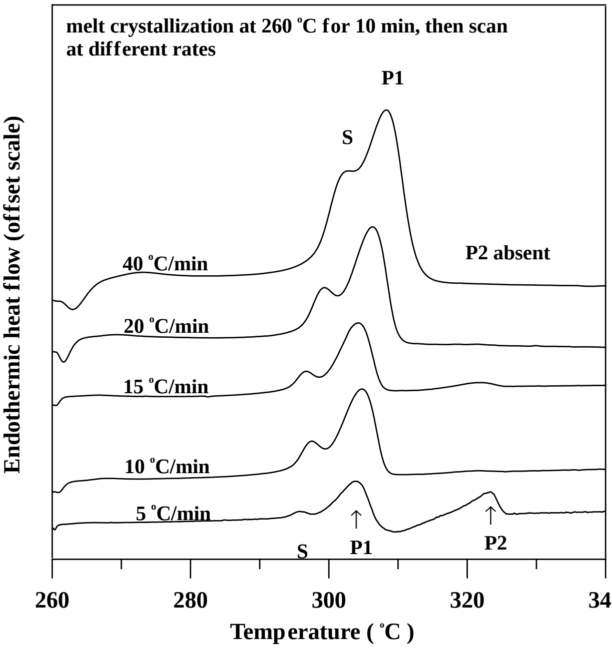

Fig. 2. DSC result of the 260°C-melt-crystallized samples scanned at various rates as indicated for each trace.

scanning rates revealed only SP1, with P2 missing. However, when compared at the same scanning rates, the relative magnitude of P2 is slightly smaller in 260°C-melt-crystallized samples than the 250°C-melt-crystallized ones. This suggests that melt-crystallization of PEDEK*m* at lower temperatures probably led to lamellar populations in SP1 that might be more available/amenable to melt/re-crystallize for packing into thicker lamellar crystal of P2.

The fact that the 250 or 260°C-melt-crystallized PEDEK*m* samples (scanned at higher rates) revealed no melting traces of P2 suggests that formation of P2 crystal may be related to scanning-rate induced changes in the previously existing P1 crystal. To compare the trends more clearly, the key transitions for the 250°C-melt-crystallized vs. 260°C-melt-crystallized samples are summarized in comparative plots as a function of scanning rate. Fig. 3 shows the apparent melting temperatures of SP1 and P2 crystal entities, for (A) 250°C-melt-crystallized, and (B) 260°C-melt-crystallized PEDEK*m* samples. For both sets of samples, the position of SP1 (low melting crystal) remained roughly constant regardless of scanning rates; however, P2 (high-melting crystal) decreases with increasing scan rate. Note the temperature location of SP1 remains roughly constant with respect to scanning rate, which suggests that the peak position is probably a balance between two competing thermal processes: (1) melting of SP1 (endothermic peak) being followed immediately with (2) re-crystallization (exothermic peak) of the melted entity. The melting/re-crystallization during scanning thus led to a newly packed crystal entity (i.e. P2). The fact that P2 decreases with higher scanning rate may be viewed as a proof that the crystal entity of P2 is likely associated with re-crystallization/re-melting of a previously existing crystal.

The enthalpies of thermal transitions in PEDEK*m* are then compared for samples melt-crystallized at different thermal histories. Fig. 4 shows the melting enthalpy of SP1 and P2 crystal entities as well as the enthalpy of crystallization that took place between SP1 and P2 thermal processes. All measured enthalpy values were plotted as a function of scanning rate used in the DSC measurements. Diagram-A is for the 250°C-melt-crystallized (2 h) samples, and Diagram-B summarizes the data for the 260°C-melt-crystallized (2 h) samples. The melting enthalpy for the originally existing SP1 crystal is seen to increase slightly with scanning rate; however, a drastically different trend is observed for the melting enthalpy of P2. A plausible explanation for the rapidly decreasing melting enthalpy of P2 is because it is for the re-crystallized species of P2 crystal, whose amount decreases rapidly with higher scanning rates. The enthalpy associated with the re-crystallization (ΔH_c) exhibits a similar trend of rapidly approaching

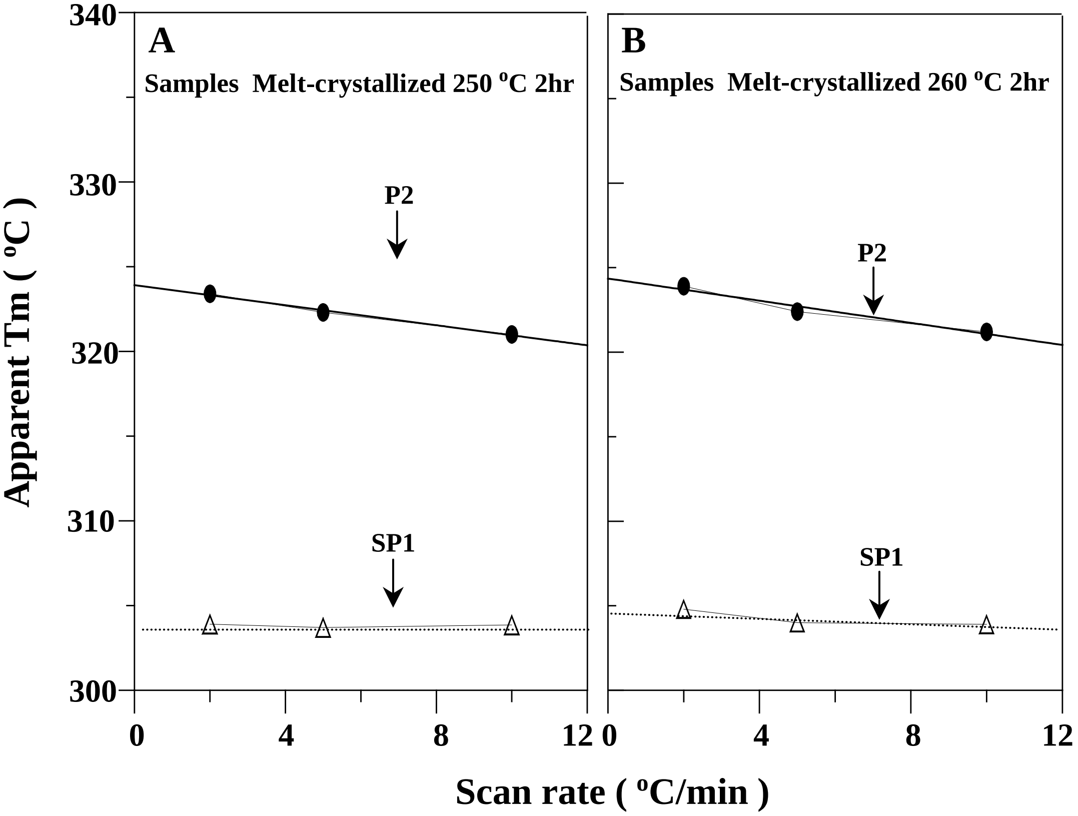

Fig. 3. Apparent melting temperatures of SP1 and P2 for (A) 250°C-melt-crystallized, and (B) 260°C-melt-crystallized PEDEK*m* samples.

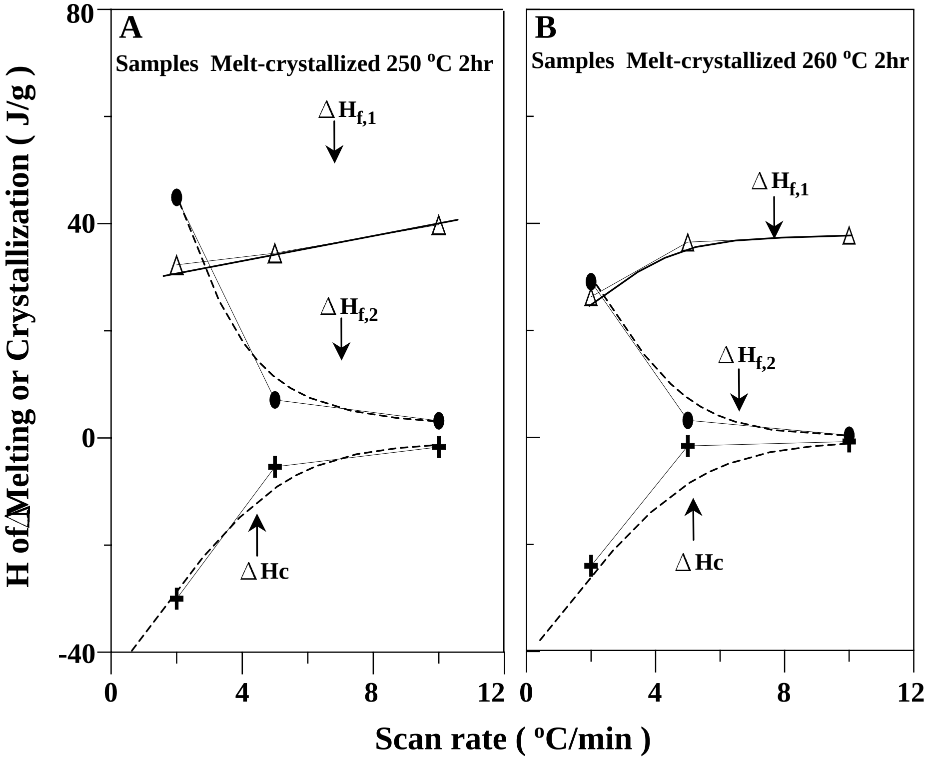

Fig. 4. Dependence of melting enthalpy of SP1 and P2 crystal and enthalpy of crystallization (between SP1 and P2) on scanning rate.

zero as the melting enthalpy of the P2 crystal ($\Delta H_{f,2}$) at increasing DSC scan rates.

To investigate the effect of crystallization time at 260°C on the crystalline/lamellar morphology and thermal behavior, a set of samples was prepared by melting the polymer (at 340°C) and allowing it to crystallize (from melt) at 260°C for different periods of time ranging from 0.5 to 60 min. All samples were scanned at the same rate of 10°C/min. The DSC traces are not shown for brevity. In addition, the $\Delta H_{f,1}$ was found to be about 52.0–52.5 J/g for all samples (260°C-melt-crystallized for various times), which suggests that the post-crystallization scanning (between 260 and 290°C at 10°C/min) tended to narrow the thickness distribution of the crystal entities of SP1 in all the samples regardless the different crystallization times previously imposed on the samples prior to the DSC scanning. The development of SP1 crystal entities, induced either by isothermal crystallization at 260°C or post-crystallization heat-scanning between 260 and 290°C, however, does not interfere with the formation mechanism of the high-melting crystal entity of P2 ($T_{m,2} = 322$°C) via the stated melting/re-packing mechanism of the SP1 crystal entities ($T_{m,1} = 296$–305°C).

Next, an additional set of samples was prepared by melting the polymer (at 340°C), letting it to melt-crystallize at a high temperature of 280°C for 1 h. The purpose was to compare the difference in the low-temperature (260°C or lower) P1 vs. high-temperature (280°C or higher) crystallized P1 morphology on subsequent melting/re-crystallization to producing crystal entity of P2. The melt-crystallized samples were then scanned all at 10°C/min from 280 to 340°C to reveal its melting transitions, from which its possible crystalline morphology was analyzed. Fig. 5 shows the DSC traces (scanned 10°C/min) for the 280°C-crystallized

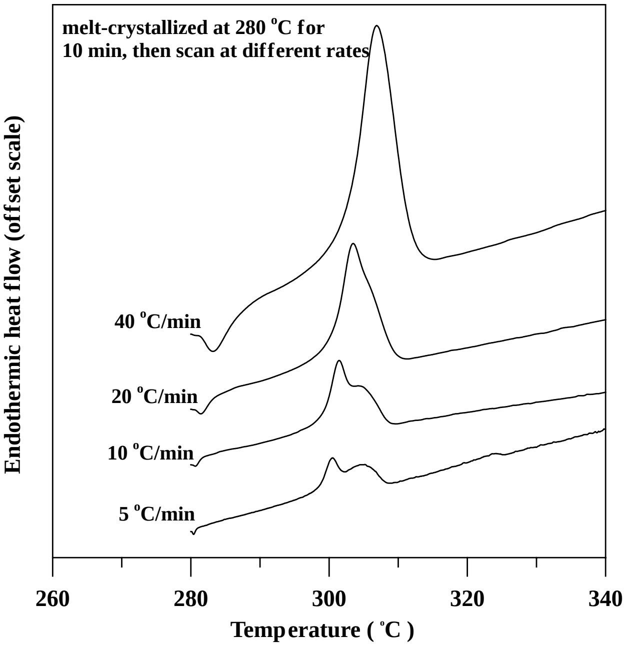

Fig. 5. DSC thermograms (10°C/min) for the 280°C-melt-crystallized samples.

samples. Interestingly, it shows only an almost merged doublet peak at 301°C ($T_{m,1}$), while the high melting peak ($T_{m,2}$) is completely invisible. The measured heat of fusion for the collective doublet SP1 endotherm was $\Delta H_{f,1} = 54.3$ J/g. As a slow-cooled sample would develop a maximum crystallinity corresponding to a heat of fusion of about 52–54 J/g, this 280°C-melt-crystallized (60 min) sample had apparently developed a nearly maximum crystallinity (which is 43 wt%, assuming 125 J/g for fully-crystalline PEDEK*m*) [3]. Obviously, the absence of crystallization exotherm at 307°C indicates that melting and re-crystallization (packing into the crystal entity to be melted again at a higher temperature) of the low-melting crystal entity (SP1) did not seem to occur. As a result of absence of high-melting crystal entity, melting of the crystal entity at 320°C (P2) did not take place and peak of $T_{m,2}$ was absent from the DSC traces.

3.2. Lamellar thickness of P1 vs. P2

To understand the relationships between the crystal entities of SP1 vs. P2, one has to clarify how the thickness distribution in P1 crystal entity may affect downstream melting of SP1 crystal and subsequent re-packing into P2 crystal. The lamellar thickness distribution of SP1 crystal entities could be significantly altered if a different isothermal temperature was used. Thermal characterization was performed on a series of samples isothermally crystallized at 150, 260, 270, 280, or 290°C to their maximum crystallinity (43–45 wt%, or $\Delta H_{f,1} = 52$–54 J/g). A very slow scanning rate (2°C/min) was used to analyze the isothermally crystallized samples, with the DSC scanning from respective crystallization temperatures. Fig. 6 shows the DSC traces (bottom to top) for: (a) 250°C, 2 h, (b) 260°C, 2 h, (c) 270°C, 3 h, (d) 280°C, 5 h, and (e) 290°C, 5 h. For all the low-temperature-crystallized (250–280°C) samples, a quite significant P2 peak (at ca. 322°C) is observed when scanned at this low rate. The same trend is seen in the endotherm of the high-melting P2 crystal for samples melt-crystallized at increasingly higher temperatures. The integrated areas (heat of fusion) of the P2 endotherms (all measured at 5°C/min) are in decreasing order: 41.5, 34.2, 25.6, 21.2, and 2.9 J/g, for the samples isothermally crystallized at increasingly higher temperatures: 250, 260, 270, 280, and 290°C, respectively. An interesting trend is seen in the high-melting P2 endotherm for the samples melt-crystallized at different temperatures. The integrated areas (heat of fusion) of the P2 endotherms (all measured at 5°C/min) decrease from 9.8, 4.1, 1.5, to 0 J/g, for the samples isothermally crystallized at 250, 260, 270, and 290°C, respectively. The experimental results suggest that for the samples crystallized at relatively lower temperatures (e.g. 250–270°C), the thickness distribution of the developed SP1 lamellae tends to contain more crystal species of thinnest lamellae (evidenced by the shoulder peak S). These thin lamellae would melt at lower temperatures (ca. 295°C) and thus can be more readily re-packed into high-melting P2 crystals. By comparison, the samples crystallized at high enough temperatures (280 or 290°C) developed a narrower and relatively a thicker P1 lamella population. Thus, they only melt at a slightly higher temperature range (ca. 304–305°C). These thicker lamellae may simply melt at slightly higher temperatures but do not have sufficient time to re-pack into the high-melting P2 crystal within the time frame of a regular scanning (10°C/min or higher). The opposite is true if the samples were scanned at low rates (e.g. 2°C/min).

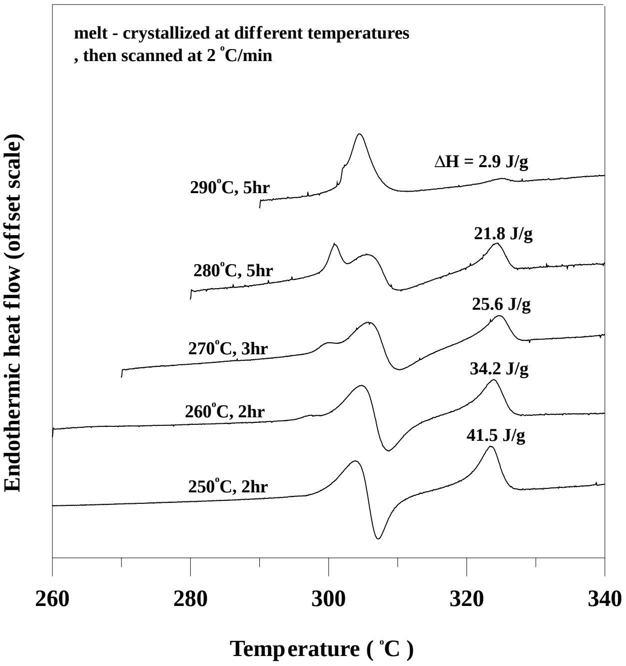

Fig. 6. DSC traces for PEDEK*m* crystallized at: (a) 250°C, 2 h, (b) 260°C, 2 h, (c) 270°C, 3 h, (d) 280°C, 5 h, and (e) 290°C, 5 h.

3.3. Further evidence of melting/re-packing

If given sufficient time at the re-crystallization (post-annealing) temperature (307–310°C), the crystallized samples might still be able to develop a significant amount of P2 crystal entities by melting the pre-existing P1 crystal and re-packing the melted polymer chains. This hypothesis was thoroughly tested, and results will be discussed in following sections. The next scheme of experiments was to investigate if or not isothermally post-annealing the 280°C-crystallized PEDEK*m* might lead to P2 lamellar packing by transforming (i.e. via melting/re-crystallizing) the previously existing P1. The 280°C-melt-crystallized samples were post-annealed at selected temperatures that were regarded as appropriate for re-packing of the melted P1 polymer chains to P2 lamellae. The first temperature chosen for post-crystallization annealing was 300°C. Note that this temperature was intended for preferentially melting the thinner S (shoulder peak) lamellae ($T_m = 295$°C) but not quite for melting the P1 species ($T_m = 303$°C). Fig. 7 shows

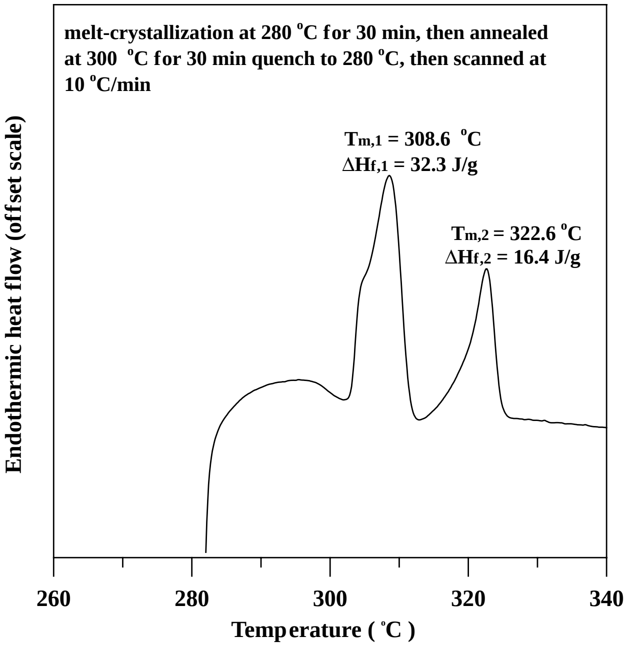

Fig. 7. Melting peaks revealed for a 280°C-crystallized sample (30 min) further post-annealed at 300°C.

the DSC result for a 280°C-crystallized sample (30 min) further post-annealed at 300°C for 30 min before it was quenched to 280°C to initiate scanning (at 10°C/min) to identify its thermal transitions, which were then analyzed to reveal their association with the developed crystalline lamellar morphology. The thermogram shows both P1 and P2, with $T_{m,1} = 308.6$°C, $\Delta H_{f,1} = 32.3$ J/g, and $T_{m,2} = 322.6$°C, $\Delta H_{f,1} = 16.4$ J/g. Note that $T_{m,1}$ (308.6°C) for the post-annealed sample is significantly higher than that found in 280°C as-crystallized sample ($T_{m,1} = 305$°C). The previous result has demonstrated that P2 melting peak may be found in 250, 260, or 270°C-melt-crystallized samples subjected to slow scanning (10°C/min or lower) in DSC. For the samples crystallized at high temperatures (e.g. 280, 290°C), there was no significant amount of thin and low-melting SP1 crystal lamellae, thus DSC scanning did not lead to thick P2 crystal via melting/re-crystallization of originally thin SP1 lamellae. However, post-annealing these higher-temperature (280 and 290°C) crystallized samples for long enough time would allow for the melted P1 crystal to slowly re-pack into P2 crystal. The result in this figure further proves that the P2 crystal entity could also be re-packed from melted P1 crystal by post-annealing the previously crystallized sample at a higher isothermal temperature (e.g. 300°C) as well as by dynamic scanning-induced melting/re-crystallization.

Next, effects of post-annealing at temperatures even higher than 300°C were further examined. As the post-melting re-crystallization was known to take place at temperatures around 305–310°C, a post-annealing temperature of 307°C was performed on 270°C-crystallized PEDEK*m*. The time of post-annealing isothermally held at 307°C was varied from 5 to 60 min. Fig. 8 shows the DSC results for the 270°C-crystallized samples (60 min) further post-annealed at 307°C for times ranging from 5 to 60 min before they were quenched down to 280°C to initiate DSC scanning (at 10°C/min) to reveal its thermal transitions in association with the developed lamellar morphology. The figure shows the intensity of P2 (at $T_{m,2} = 325$°C) increases at the decrease of P1 (at $T_{m,1} = 301$–306°C) with increasing post-anneal time at 307°C. The $\Delta H_{f,2}$ (heat of fusion for P2) increases from 0 to about 37.4 J/g, while $\Delta H_{f,1}$ (heat of fusion for P1) decreases from 54 J/g to about zero for the annealing times increasing from 0 to 60 min. Note that $T_{m,2}$ (ca. 326°C) for the 307°C-post-annealed samples is higher than that found in melt/re-crystallized samples (ca. $T_{m,2} = 322$°C) upon DSC scanning. The result further supported that the originally low-melting crystal of P1 (in 270°C-crystallized samples) was melted at 307°C but re-crystallize slowly into the P2 crystal of a larger thickness and higher melting, as long as sufficient time was allowed at 307°C.

3.4. Direct P2 crystal growth from melt

Other possible mechanisms for the high-melting crystal entity of P2 in PEDEK*m* needed to be examined. Other than the mechanism through melting and re-packing of the originally thin lamella (i.e. SP1), one would be interested in knowing whether the liquid polymer chains could be directly packed into P2, without via melting and re-packing the originally thin lamellae. An additional set of four samples was prepared by melting the polymer (at 340°C) and allowing it to crystallize (from melt) at 307°C (in DSC

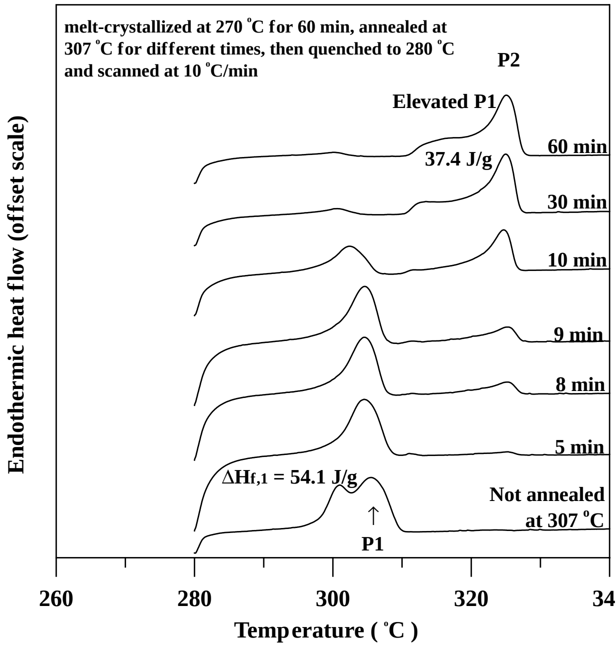

Fig. 8. Melting peaks for the 270°C-crystallized samples (60 min) further post-annealed at 307°C for times ranging from 5 to 60 min.

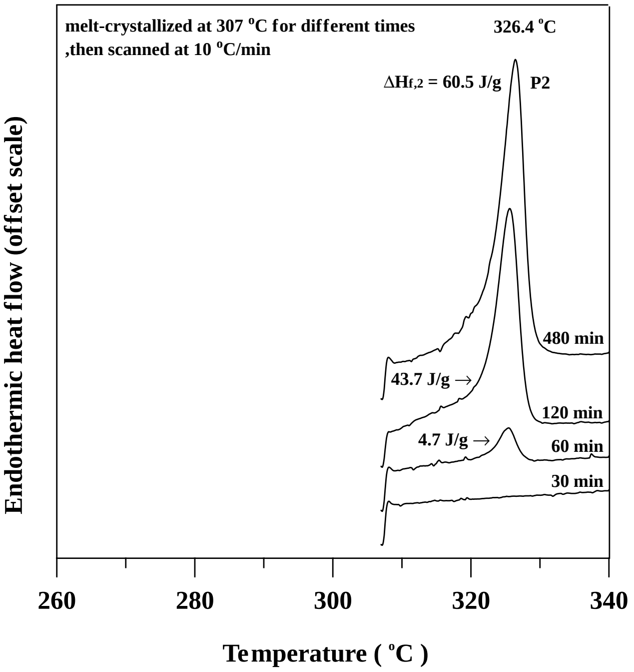

Fig. 9. DSC traces (10°C/min) for the samples melt-crystallized at 307°C for 30, 60, 120, or 480 min, (from bottom to top), respectively.

cell) for different periods of times: 30, 60, 120, and 480 min, respectively. These melt-crystallized samples were then all scanned in DSC at the same rate of 10°C/min, respectively, from 307 to 340°C to reveal their thermal transitions. Note that the samples were not quenched from 307°C to a lower temperature to initiate DSC scanning but were scanned directly from the isothermal holding temperature of 307°C; the purpose was to eliminate any scanning-induced changes of already fixed crystalline morphology in the crystallized samples. Fig. 9 shows the DSC traces (10°C/min) for the samples melt-crystallized at 307°C (in DSC cell) for 30, 60, 120, or 480 min (bottom to top), respectively. Apparently, the thermal analysis demonstrated that packing of thickened P2 lamellae directly from liquid PEDEK*m* polymer chains was possible, but direct melt-crystallization of P2 at 307°C proceeded much more slowly in comparison to that of crystallization at lower temperatures leading to thinner P1 lamellae. The result shows that up to 30 min at 307°C still did not lead to any significant amount of P2 crystal, and the DSC results revealed only a flat baseline (i.e. $\Delta H_{f,2} = 0$). Note that the measured heat of P2 fusion ($\Delta H_{f,2} = 0$) reflects the amount of P2 crystal packed at 307°C-melt-crystallization. The $\Delta H_{f,2}$ apparently increases with time of crystallization at 307°C: 0, 4.7, 43.7, and 60.5 J/g for crystallization time of 30, 60, 120, and 480 min, respectively. All 307°C-crystallized PEDEK*m* is populated with thick P2 crystal entity, but none of P1 crystal, which is the main morphology for samples crystallized at temperatures below the shoulder peak (shoulder preceding P1) temperature of ca. 295°C. The maximum crystallinity achieved in 307°C-crystallization is higher than that for the P1-populated samples (crystallization below 295°C). The maximum $\Delta H_{f,1}$ is about 54 J/g, or 43 wt% crystallinity (mainly P1 crystal); but the maximum $\Delta H_{f,2}$ is about 61–62 J/g, equivalent to almost 50 wt% crystallinity (primarily P2 crystal).

X-ray diffraction was performed to discern the unit cell packing in the samples melt-crystallized at three representative temperatures: 260, 280, and 310°C. Fig. 10 shows the X-ray diffractograms for the samples pre-melted at 340°C to liquid and quickly quenched to an isothermal crystallization temperature: (a) 250°C, 2 h, (b) 260°C, 2 h, (c) 270°C, 3 h, (d) 280°C, 5 h, and (e) 290°C, 5 h. After the thermal treatments at the intended temperature, they were then quenched to ambient to preserve its developed morphology for WAXD analysis. All samples showed four major diffraction peaks (for 110, 113, 200, and 215 planes, respectively) at exactly the same angles. A 307°C-crystallized sample (for 5 h) was also analyzed using WAXD, and the result revealed same unit cell packing as that found in the samples crystallized at below 290°C. The different lamella thickness and distributions in the various melt-crystallized samples of PEDEK*m* is basically packed by the same unit cell of orthorhombic packing, i.e. $a = 0.785$ nm, $b = 0.605$ nm and $c = 4.77$ nm [3].

A sample was prepared by treatment to melt-crystallization at 307°C, which was chosen because it was the peak temperature of the crystallization exotherm during DSC

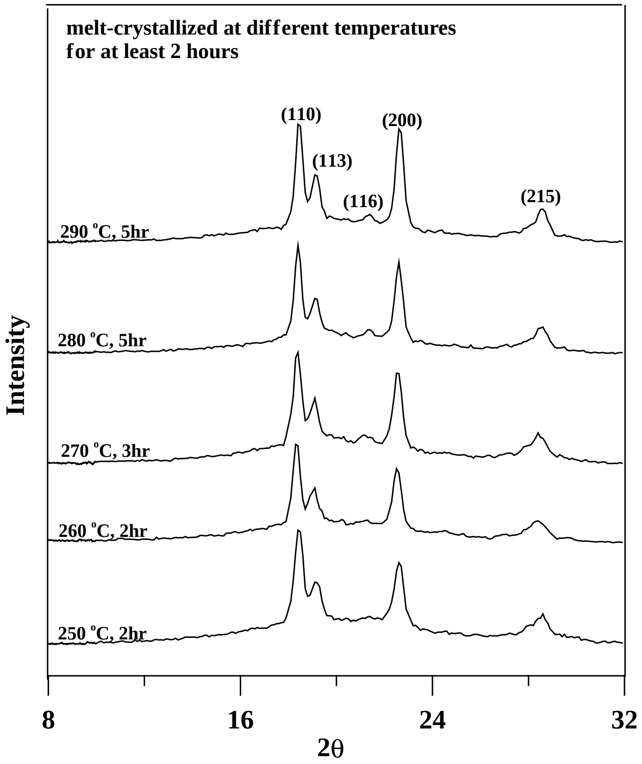

Fig. 10. X-ray diffractograms for PEDEK*m* pre-melted at 340°C and quenched to crystallize isothermally at: (a) 250°C, 2 h, (b) 260°C, 2 h, (c) 270°C, 3 h, (d) 280°C, 5 h, or (d) 290°C, 5 h.

Fig. 11. SEM graph revealing the branched and thickened lamellae in PEDEK*m* melt-crystallized at 307°C for 5 h.

scanning. To ensure full development of crystalline morphology at 307°C directly from melt, a long time of 5 h was allowed. Fig. 11 shows the SEM photograph revealing the thickened lamellar morphology in PEDEK*m* melt-crystallized at 307°C for 5 h. Interestingly, the lamellar morphology for the 307°C-melt-crystallized PEDEK*m* sample is dramatically different from those seen in the samples melt-crystallized at 290°C or lower. The lamellae are significantly thickened and branched. If isothermally crystallized at temperatures higher than 295°C and held to full maximum crystallinity, only P2 lamellae were found, which are significantly more thickened and branched than the P1 crystal. The thickened lamellae are less inclined to aggregate in straight bundles; instead, they appear as branched lamellae. The many branches of lamellae were obviously a result of lamellar thickening that developed during the high-temperature melt-crystallization of PEDEK*m* at 307°C. It would be of interest to compare these two types of crystalline morphology in melt-crystallized PEDEK*m* with those found in other polyaryletherketone polymer systems. Lovinger et al. [20] and Cheng and co-workers [5] have reported a 'two-eye' spherulitic structure in melt-crystallized PEEK or poly(ether ketone ketone) with terephthalic/isophthalic (PEKK(T/I)) systems. The prevailing morphology of isolated P2 crystal in PEDEK*m* melt-crystallized at above 300°C, by contrast, is uniquely and dramatically different from two-eye lamellae.

Interestingly, Wang et al. [11] performed small-angle X-ray scattering (SAXS) reported a roughly steady increase in lamellar thickness from ca. 3 to 5.5 nm when PEDEK*m* was annealed at 230–290°C. They claimed a 'jump-like' increase in lamellar thickness at annealing temperature of 260°C. This, however, is misleading. As a quenched glassy PEDEK*m* (originally amorphous) is scanned in DSC, it exhibits two crystallization exotherms ($T_{c,1} = 225°C$, $T_{c,2} = 260°C$). One may be easily misled to interpret the lamella data as PEDEK*m* exhibits a second crystallization exotherm at 260°C. We performed POM characterization on PEDEK*m* samples crystallized at temperatures between 220 and 310°C. The morphology of PEDEK*m* samples was all of a regular spherulitic pattern with similar lamellar bundles when the samples were crystallized between 220 and 290°C. In other words, the lamellar thickness may steadily increase within the temperature range of 220–290°C, but there is unlikely a break jump in the lamellar thickness owing to either one of the series crystallizations at 225 or 260°C. On the other hand, as PEDEK*m* was melt-crystallized at 300–310°C, a very different crystalline morphology was found. POM characterization on a 307°C-melt-crystallized PEDEK*m* revealed that the Maltese-cross-pattern and spherulitic morphology both disappeared and the morphology could no longer be claimed a regular spherulite. The morphology was somewhat similar to 'axialites' found in a Regime-I growth mechanism. A cut-off temperature that signifies a break-jump in the lamellar thickness is actually ~307°C that determines which of two drastically different types of lamellae thickness in melt-crystallized PEDEK*m*. The cut-off temperature of 307°C roughly coincides with the third crystallization peak ($T_{c,3}$) that is located between the P1 and P2 melting peaks. Bassett et al. [21] have also reported axialites in isotactic polystyrene (iPS, melt-crystallized at 220°C), and suggested that polymer spherulites can form independently of the mechanism of Keith and Padden [22].

3.5. Overall discussion

Multiple melting in semicrystalline polymers is usually attributed to two mechanisms. Most investigators argue that these two mechanisms are mutually exclusive. This study, using PEDEK*m* as an ideal model, has demonstrated that the melting behavior in a semicrystalline polymer may be a result of both kinds of mechanisms to different extents depending on thermal histories, scanning rate, time and temperature of post-annealing. The first of these two mechanisms proposes polymorphism, with each of the crystals giving $T_{m,1}$ and $T_{m,2}$, respectively. Typically, as a quenched glassy PEDEK*m* (initially amorphous) is scanned at ~10°C/min or higher, two crystallization exotherms in series are observed ($T_{c,1} = 225°C$, $T_{c,2} = 260°C$), and the series crystallization at 225 and 260°C developed only a low-melting P1 crystal. Similarly, the PEDEK*m* melt-crystallized at low temperatures (300°C or below) would develop predominantly low-melting P1 crystal with no or little P2 crystal, while melt-crystallization at 300–307°C would develop the high-melting P2 crystal with no or very little P1 in the spherulites at all. A dynamic cooling of PEDEK*m* from the molten state can in principle develop both co-existing P1 and P2 crystals of different proportions depending on the cooling rate. The cooled PEDEK*m* samples, when scanned in DSC, would reveal two melting peaks regardless of reorganization.

The second of these two mechanisms that contributes to multiple (dual) melting in PEDEK*m* involves re-organization of thinner lamellar crystals into thicker ones. Either the case of two co-existing crystals (P1 and P2) or the case of melting/re-crystallization transformation in PEDEK*m* would lead to sequential appearance of dual melting peaks. Interpretation of multiple melting in semicrystalline polymers must take both mechanisms into consideration. Both P1 and P2 crystals could co-exist in PEDEK*m* only if the samples were intentionally crystallized partially first at higher 295°C, then at lower than 290°C. Similarly, if PEDEK*m* was dynamically cooled from melt at slow rates, various proportions of P1/P2 may be developed depending on the cooling schemes. Kinetically, P2 lamellae could be packed only at higher temperatures (300–310°C) and grow much more slowly than the P1 crystal would at lower temperatures (250–290°C). In addition, the maximum crystallinity (50 wt%) achieved in the P2-dominated PEDEK*m* sample is higher than that for the P1-populated samples (43 wt%). Furthermore, for crystallization below 290°C, the thickness distribution of packed lower-melting SP1 (or P1) lamella varied depending on crystallization temperature, and this variation led to different behavior of downstream melting/re-crystallization of P1 crystal into P2 crystal. When melt crystallization of PEDEK*m* was performed at moderate temperatures (e.g. 240–260°C), the liquid polymer chains were packed into a wide distribution of SP1 lamellae, containing a good fraction of thinner lamellae. The thickness-distributed lamellae upon melting would exhibit a lower-melting doublet endotherm (SP1 of $T_{m,1}$). The thinnest lamellae (S) melt at a lower temperature of 295°C (the shoulder peak of the doublet melting), but can be more readily re-packed into thicker lamellar entities at about $T_c = 307$°C, which are to be melted again at 322°C upon subsequent scanning. Post-annealing at an isothermal temperature was found to have similar effects to that of dynamic scanning. If the 260°C-crystallized samples were further held at 307°C for different periods of time, the thinner SP1 lamellae of $T_{m,1}$ would be gradually transformed into thick P2 lamellae of $T_{m,2}$. The amount transformed was proven to increase roughly in proportion to the time at 307°C. When melt crystallization of PEDEK*m* was performed at moderately higher temperatures (280–290°C), the liquid polymer chains were packed into a narrow distribution of thicker lamellae, containing a smaller fraction of thinner lamellae and larger fraction of thick lamellae. The amount of low-melting thin lamella available for melting and re-crystallization at 307°C is comparatively less. Thus, upon DSC scanning of these crystallized samples, no high-melting crystal was formed by melting/re-crystallization mechanism. However, if post-annealing at 300–310°C for long enough time was imposed on these melt-crystallized samples prior to DSC scanning, high-melting crystal (P2 of $T_{m,2}$) could be formed.

4. Conclusion

DSC scanning on melt-crystallized PEDEK*m* at low rates would reveal two melting endotherms at 302 and 322°C in series appearance, which are associated with two distinctly different lamellar populations, P1 and P2, respectively. Melt-crystallization at below 300°C (e.g. 250, 260, 270, 280, or 290°C) led to predominantly low-melting P1 crystal, while mainly high-melting P2 crystal entity if samples were melt-crystallized at above 300°C (e.g. 300, 307, or 310°C). That is, the P1 and P2 crystals do not necessarily co-exist in melt-crystallized PEDEK*m* although DSC scanning reveals two melting peaks in the sample. Isothermally crystallized (300°C or lower) samples possess only P1 (or SP1) lamella crystal, which may undergo further melting/re-crystallization to partially or completely transform to P2, giving two endothermic melting peaks and a crystallization exotherm between these two melting peaks. As P1 crystal is further melted and recrystallized into P2, a third crystallization exotherm ($T_{c,3}$) was found at about 307°C that is between the P1 and P2 melting peaks. However, if PEDEK*m* is isothermally crystallized at temperatures higher than ~300°C to full maximum crystallinity, only P2 crystal exists, giving only $T_{m,2}$, with no trace of P1.

Regardless of the drastically different lamellar entities in PEDEK*m* when subjected to different thermal histories, no difference in the unit cell was found, and the unit cell remained orthorhombic packing with the same *a*, *b*, *c* dimensions, which is in agreement with an earlier report by Wang et al. [11]. This is a different finding from those reported by Blundell et al. [3] or Rueda et al. [10] who have concluded dramatic changes in crystal unit cell dimensions in PEDEK*m* (PK99) or an oligo(aryl ether ketone), respectively. A cut-off temperature that signifies a break-jump in the lamellar thickness is actually ~307°C that determines which of two drastically different types of lamellae thickness in melt-crystallized PEDEK*m*. Interestingly, the cut-off temperature of 307°C roughly coincides with the third crystallization peak ($T_{c,3}$) that is located between the P1 and P2 melting peaks.

Acknowledgements

This work is generously supported by Taiwan's National Science Council, to which the authors express their sincere gratitude for Grant of #NSC89-2206 E006-015.

References

[1] Gardner KH, Hsiao BS, Matheson Jr RR, Wood BA. Polymer 1992;33:2483.

[2] Gardner KH, Hsiao BS, Matheson Jr RR, Faron KL. Polymer 1994;35:2290.

[3] Blundell DJ, Liggat JJ, Flory A. Polymer 1992;33:2475.

[4] Cheng SZD, Ho RM, Hsiao BS, Gardner KH. Macromol Chem Phys 1996;197:185.

[5] Ho RM, Cheng SZD, Hsiao BS, Gardner KH. Macromolecules 1995;28:1938.

[6] Ko TY, Woo EM. Polymer 1996;37:1167.

[7] Marand H, Prasad A. Macromolecules 1992;25:1731.
[8] Zolotukhin MG, Rueda D, Andre I, Ripoll MM, Abajo DJ, Alvarez JC. Macromol Chem Phys 1997;198:2089.
[9] Rueda DR, Garcia MC, Gutierrez Ania F, Zolotukhin MG, Balta Calleja FJ. Macromolecules 1998;31:8201.
[10] Rueda DR, Zolotukhin MG. Macromol Chem Phys 1997;198:3517.
[11] Wang S, Wang J, Zhang H, Wu Z, Mo Z. Macromol Chem Phys 1996;197:1643.
[12] Blundell DJ, Newton AB. Polymer 1991;32:308.
[13] Olley RH, Bassett DC, Blundell DJ. Polymer 1986;27:344.
[14] Lovinger AJ, Hudson SD, Davis DD. Macromolecules 1992;25:1752.
[15] Wunderlich B. Macromolecular physics, vol. 3. New York: Academic Press, 1976.
[16] Blundell DJ. Polymer 1987;28:2248.
[17] Lee Y, Porter RS. Macromolecules 1987;20:1336.
[18] Sun YS, Woo EM. Macromolecules 1999;32:7836.
[19] Liggat JJ, Staniland PA. Polym Commun 1991;32:450.
[20] Lovinger AJ, Davis DDJ. Appl Phys 1985;58:2843.
[21] Bassett DC, Vaughan AS. Polymer 1985;26:717.
[22] Keith HD, Padden Jr FJ. J Appl Phys 1963;34:2409.